International Journal of Wildland Fire
doi: 10.1071/WF20163_AC

Supplementary material

Prescribed fire and fire suppression operations influence wildfire severity under severe weather in Lassen Volcanic National Park, California, USA

Lucas B. Harris[A,E], Stacy A. Drury[B], Calvin A. Farris[C] and Alan H. Taylor[D]

[A]Department of Geography, The Pennsylvania State University, 302 Walker Building, University Park, PA 16802, USA.

[B]USDA Forest Service, Pacific Southwest Research Station, Davis, CA 95618, USA.

[C]National Park Service Fire Management, Pacific West Region, Klamath Falls, OR 97601, USA.

[D]Department of Geography, Earth and Environmental Systems Institute, The Pennsylvania State University, 302 Walker Building, University Park, PA 16802, USA.

[E]Corresponding author. Email: lbh146@psu.edu

Table S1. Comparison of vegetation types in 1935 and 2004.

Contingency table comparing vegetation types in 1935 and 2004 by area (in ha) across the study area. Abbreviated vegetation type names correspond with the full names in row one.

1935 types	B	H	SH	JP	WF	RF	LP	R	**1935 total (ha)**
barren	10	0	0	32	4	10	6	1	**63**
herbaceous	1	9	0	0	5	9	45	0	**69**
shrubland	7	4	44	44	109	334	34	1	**577**
Jeffrey pine	80	28	38	278	902	2149	411	0	**3886**
white fir	0	0	0	0	0	28	0	0	**28**
red fir	21	1	24	0	17	701	104	4	**872**
lodgepole pine	31	56	15	26	35	516	882	2	**1563**
riparian	1	1	0	0	2	10	10	0	**24**
white pine	9	0	7	0	0	431	57	0	**504**
2004 total (ha)	**160**	**99**	**128**	**380**	**1074**	**4188**	**1549**	**8**	**7586**

Table S2. Spearman rank correlations (r_s) between fire severity (tree basal area loss), daily area burned and daily weather (n = 19 days).

Stars represent significance based on a Holm-Bonferroni correction: *< 0.05, **<0.01, ***<0.001.

Variable	Basal area loss	Area burned
Maximum temperature	0.30	0.46
Minimum relative humidity	-0.71**	-0.56*

Energy Release Component	0.52	0.80***
Wind speed	0.29	0.01

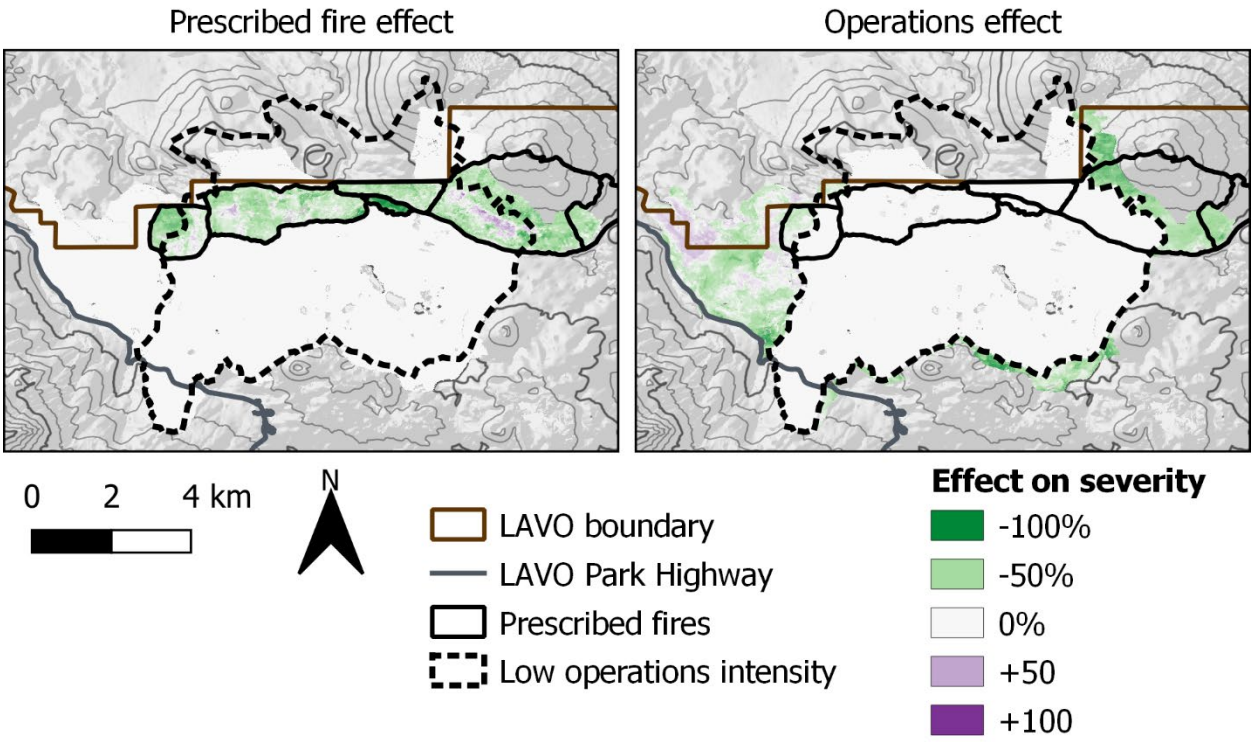

Fig. S1. Separate maps of the effects of treatment and operations on the severity of the Reading Fire, i.e., the proportional differences between fire severity predictions with and without prescribed fire and operations. Areas beyond (within) the black line experienced moderate–high (low) intensity of fire suppression operations.

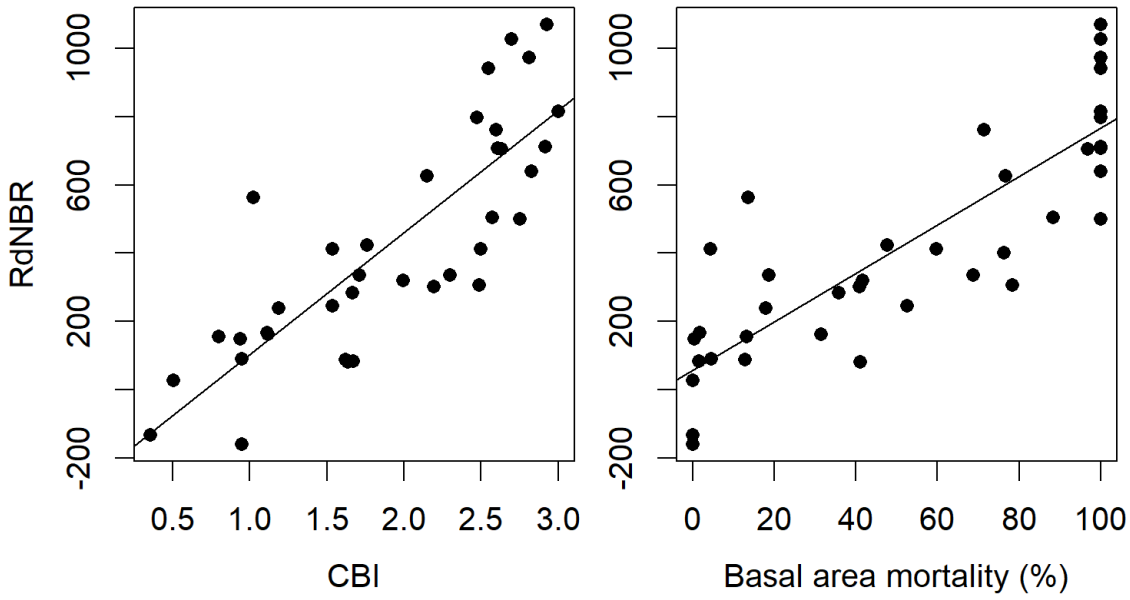

Fig. S2. Comparison between two field-based fire severity measures, the composite burn index (CBI, $R^2 = 0.68$) and tree basal area loss ($R^2 = 0.72$), and the Relativized differenced Normalized Burn Ratio (RdNBR) at each field plot surveyed in 2013 (n = 39) with linear regressions shown.

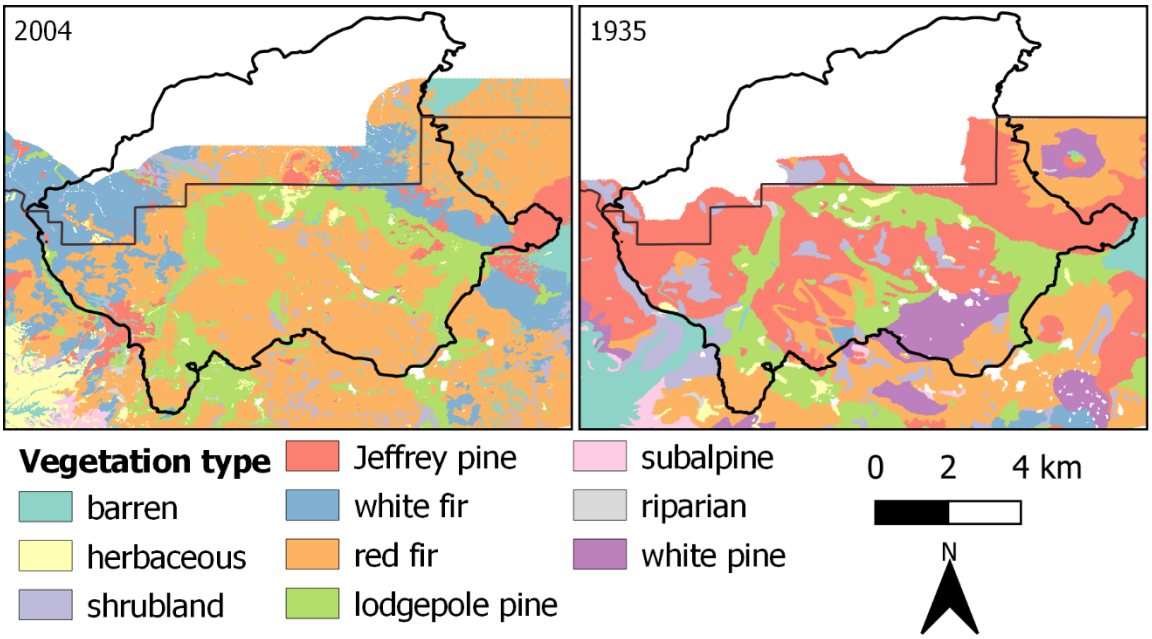

Fig. S3. Vegetation type layers used in the Reading Fire analysis, representing 2004 and 1935 conditions. The Reading Fire perimeter is shown along with the northern boundary of Lassen Volcanic National Park.

Field data on fire severity and comparison with prior work

In addition to quantifying tree mortality due to wildfire by basal area (BA loss), we also assessed the Composite Burn Index (CBI, Key and Benson 2006) in our field plots following standard protocols. Specifically, we visually assessed fire effects in four strata: herbs, low shrubs and trees < 1 m tall; tall shrubs and trees, intermediate-sized trees, and trees > 29.5 cm dbh. Factor scores were averaged within each stratum, and then the stratum scores were averaged to calculate the total plot CBI on a scale of 0 (no fire effects) to 3 (highest severity). We obtained the following linear relationship between CBI and RdNBR:

$CBI = 1.11 + 0.00189*RdNBR$ ($R^2 = 0.68$)

The strength of our relationships between RdNBR and BA loss compares favorably with those developed for 25 California fires by Miller et al. (2009). In forested areas, they obtained $R^2 = 0.53$ for BA loss and $R^2 = 0.68$ with the Composite Burn Index (CBI, Key and Benson 2006). Although prior studies in California forests have used nonlinear regression models to produce the best fits between RdNBR and field-based fire severity metrics (Miller *et al.* 2009; Koontz *et al.* 2020), scatterplots of our fire severity metrics instead suggested linear relationships (Fig. S2). The stronger correlation we obtained between BA mortality and RdNBR ($R^2 = 0.72$), compared with both the Miller et al. analysis and our CBI data, may arise from the typically dense pre-fire forest cover within the Reading Fire. CBI accounts for both understory and overstory fire effects, and therefore may correlate more strongly with RdNBR in areas of sparser tree canopy cover in which change in aerial cover of understory plants factors more strongly into RdNBR (Miller *et al.* 2009). Within dense forest, a metric like BA mortality that accounts primarily for overstory change may better reflect aerial change in vegetation cover and therefore RdNBR.

We compared BA loss and CBI for the Reading Fire using the regression models from our field data and the equations from Miller et al. (2009). For both metrics, the distribution of high-severity fire predicted by each equation was nearly identical (Fig. S4 and S5). However, the Miller et al. (2009) equations produced a bimodal distribution of CBI and BA loss including a high proportion of near-zero values. By contrast, our regression models predicted few areas with near-zero values and a greater proportion of intermediate values for both metrics (Fig. S4 and S5). This comparison shows that the regional-scale regression models of Miller et al. (2009) performed well at identifying areas of high-severity fire in the Reading Fire but underpredicted fire severity in other locations.

Because CBI was strongly correlated with BA loss in the field plots (r = 0.93, Pearson correlation), we expected that substituting CBI for BA loss in the RF model of fire severity would yield a highly similar model. Indeed, a model using CBI as the response variable instead of BA loss had the same accuracy (pseudo-r^2 = 0.53) and highly similar variable importance and partial dependence plots (Fig. S6) as the BA loss model presented in the main text.

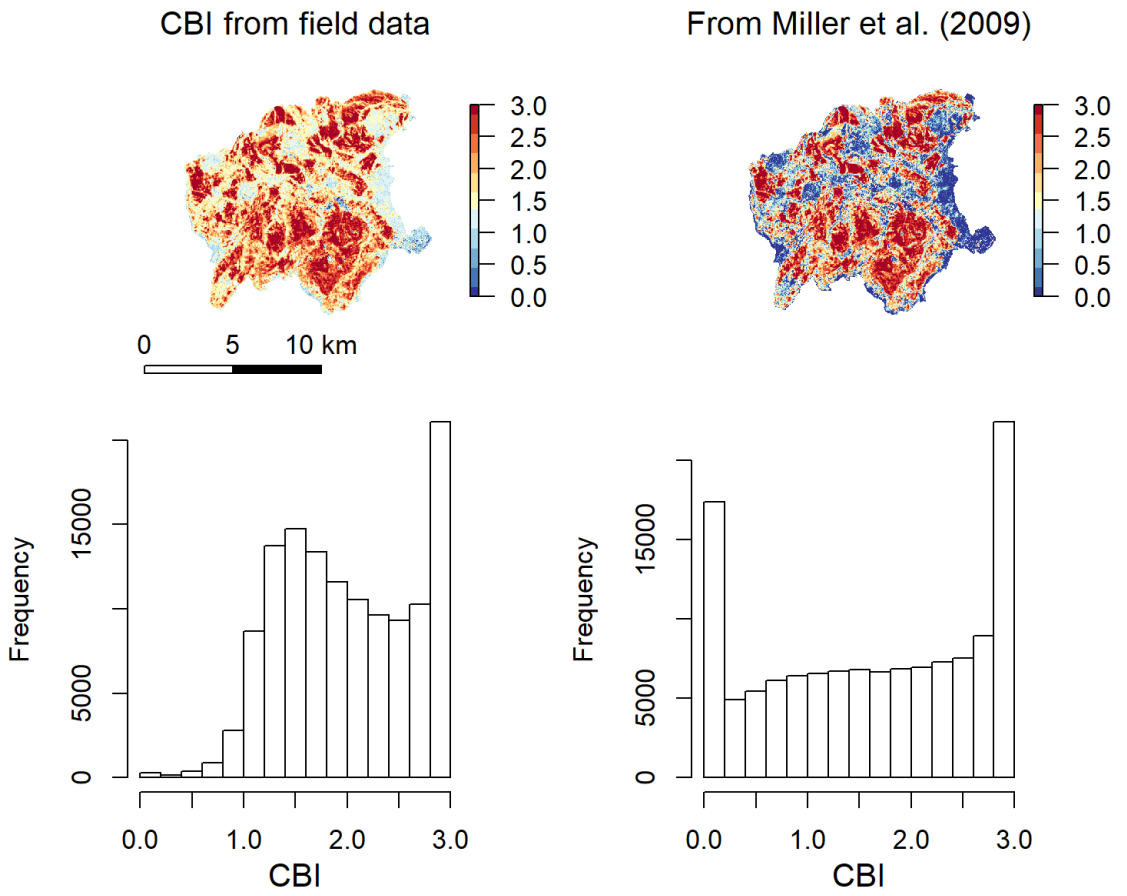

Fig. S4. Maps and histograms of the composite burn index (CBI) as calculated based on field data from the Reading Fire (left panels) and the equations developed by Miller et al. (2009, right).

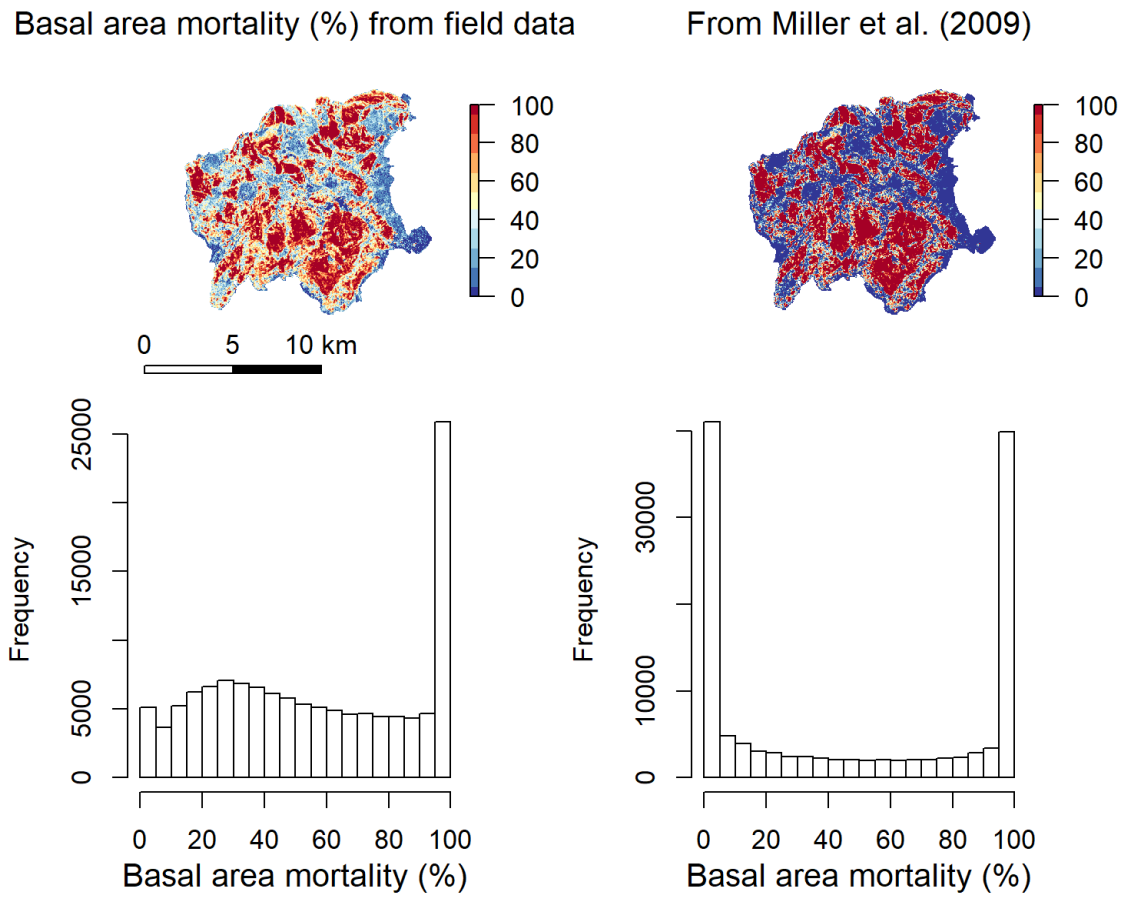

Fig. S5. Maps and histograms of percent basal area mortality as calculated based on field data from the Reading Fire (left panels) and the equations developed by Miller et al. (2009, right).

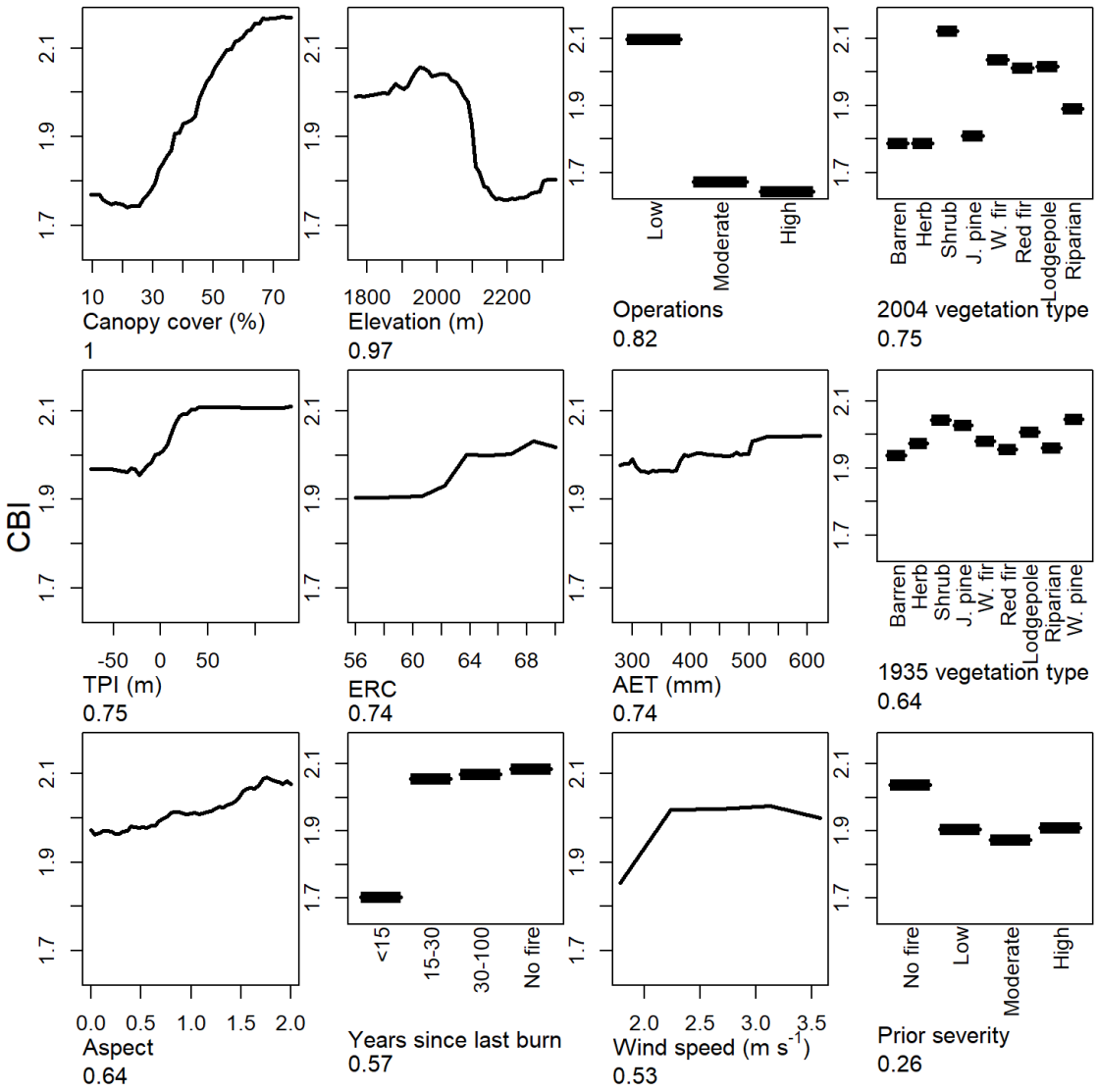

Fig. S6. Partial dependence plots showing relationships between the Composite Burn Index (CBI) from the 2012 wildfire and individual predictor variables, based on a random forest model (pseudo-r^2 = 0.53) trained with samples spaced 120 m apart. Variable importance is shown below each variable name.

Summary of weather and fire suppression operations

The initial management strategy was to confine the Reading Fire to a predetermined area bounded by the natural barriers and the park highway. Prior to 5 August, the Reading Fire spread slowly under moderate weather in high elevation terrain. From 23 July to 3 August fire spread was monitored by hand crews while they prepared the park highway to hold the fire (Fig. 4). On 4 and 5 August engine crews and hand crews worked to suppress spot fires across the highway and reduce heat near the highway using water.

On August 6 a major wind event pushed the fire across the highway and resulted in rapid spread northward in the Hat Creek drainage (Fig. 2 and 3). 6 August also marked an increase in fire severity: daily mean BA loss was < 41% up through 6 August, but > 55% from 6–11 August. An Incident Management Team (IMT) and additional resources were ordered on 6 August (initially a Type II IMT, then later a Type I IMT). Hand crews constructed hand line along the western flank of the fire between 6 and 7 August in an unsuccessful effort to keep the fire from spreading into the Raker Peak area. Other direct suppression efforts were limited during this time due to lack of resources and the location of the fire in designated wilderness with few natural fuel breaks.

By August 8 the fire had burned across the boundary into the Lassen National Forest and during the next three days made major plume-dominated runs. In fact, the majority of the fire spread within LAVO occurred between 9–11 August (64% of area burned). ERC was rising steadily throughout the period of the fire due to warm and dry conditions, and reached 96th percentile values by 11 August (based on 1990-2019 ERC values for 23 July–26 August at the Manzanita Lake weather station within LAVO). Operations during this period were focused on establishing indirect fire lines to the north to protect the nearby community of Hat Creek and

conduct firing operations (utilizing a combination of new dozer lines and existing road network), utilizing aerial operations (water and retardant) to the west and backfiring to reduce fire intensity and spread (to prevent a head fire), and monitoring to the east and south in the LAVO wilderness. Limited aerial attack occurred due to the rapid rate of spread.

After 11 August, daily fire growth and severity decreased despite high ERC values (Fig. 2). On 12 August the first major burnout operations began. On the northern perimeter firing was conducted from indirect fire lines south toward the main front, and on the western perimeter firing was used to connect to the park highway and constructed fire lines. Fire line construction and improvement and aggressive burnout and backfiring continued through 17 August with significant aerial support and ground crews. During this same period, hand crews were constructing direct line along the southern perimeter in wilderness with limited burnout and helicopter water support. The primary activity after 18 August consisted of perimeter mop-up (and some interior aerial work) to reduce hot spots and spotting. Approximately 14 km of fire perimeter in roadless areas was left unlined, but ground and aerial resources were used prevent new head fire establishment. Approximately half of that perimeter had burned into natural barriers or recent prescribed and wildland fire burn scars, which limited subsequent fire activity (Fig. 3).

Of the three zones of operations intensity shown in Fig. 4, we estimate that the “high-intensity” zone had 550 ha of backfiring, 3260 ha of burn out and approximately 600 ha was managed using aerial retardants and water to check fire spread. The “moderate-intensity” zone had 600 ha of backfiring, 50 ha of burnout and 273 ha of helicopter and ground crew mop-up and direct line. The “low-intensity” zone experienced minimal suppression operations including largely ineffective bucket work.

Notes on spatial autocorrelation and variable selection

To examine the potential influence of spatial autocorrelation on our statistical model, we ran the RF model using training datasets based on different sampling distances between points (Table S3). We examined Moran's I correlograms of residuals from these models and assessed whether autocorrelation was significant at each lag distance using 1000 permutations under the null using the 'ncf' R package (Bjornstad 2020). As has been documented in other analyses of fire severity, shorter sample spacings yielded more accurate models (Kane *et al.* 2015; Harris and Taylor 2017). Higher accuracy could result from a larger sample size providing a better representation of the variables used in the model, but could also result from pseudoreplication due to having many highly similar, nearby sample points (van Mantgem *et al.* 2001; Kane *et al.* 2015).

Table S3. Number of sample points (n) and model accuracy (pseudo-r^2) of random forest models based on different spacing between samples.

Distance (m)	n	Pseudo-r^2
120	5152	0.523
150	3269	0.473
180	2264	0.457
210	1661	0.424
240	1280	0.385
270	995	0.380
300	799	0.356
330	670	0.328
360	553	0.331
390	479	0.240

Although residuals were significantly clumped over lag distances up to 400 m, Moran's I values were still low (≤ 0.25), which suggests that the influence of spatial autocorrelation on model results is low and therefore that pseudoreplication was unlikely to strongly influence our interpretations from the model. Moran's I values using 120 m spacing were slightly greater at similar lag distances than those reported in the fire severity analyses by Kane *et al.* (2015) at 90 m spacing and by Povak *et al.* (2020) for 270 m spacing, and between values using 90 m and 180 m spacing reported by Taylor *et al.* (2020). Spatial autocorrelation among model residuals was also similar using sampling distances of 120–300 m (Fig. S7), and beyond 300 m low sample size may have led to decreased model accuracy because predictor variables were not adequately represented (Table S3). In addition, partial dependence plots from a model with 330 m spacing were highly similar to the model with 120 m spacing presented in the main text (compare Fig. S8 with Fig. 6), which shows that the shape of the relationships between fire severity and the other variables was not strongly affected by the choice of sampling distance.

We removed CWD from the statistical model of fire severity due to the shape of its partial dependence plot. Fig. S9 shows partial dependence plots for all variables from a random forest model identical to the one presented in the main text except for the inclusion of CWD. Note that the partial dependence plots and variable importance are highly similar between the two models (compare Fig. S9 with Fig. 6), which shows that the two models are similar. However, the partial dependence plot for CWD defied ecological interpretation and suggested that the RF model was overfitting with respect to the relationship between CWD and BA loss.

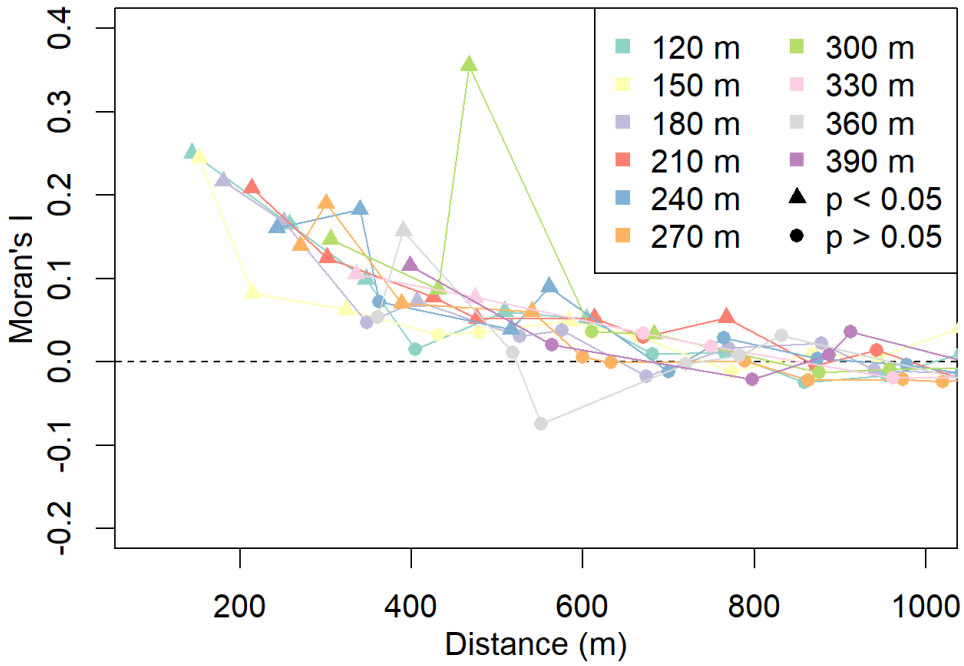

Fig. S7. Moran's I correlogram of model residuals showing spatial autocorrelation at different lag distances based in models training using gridded sample points with distances from 120-390m. Triangles denote significant ($p > 0.05$) autocorrelation.

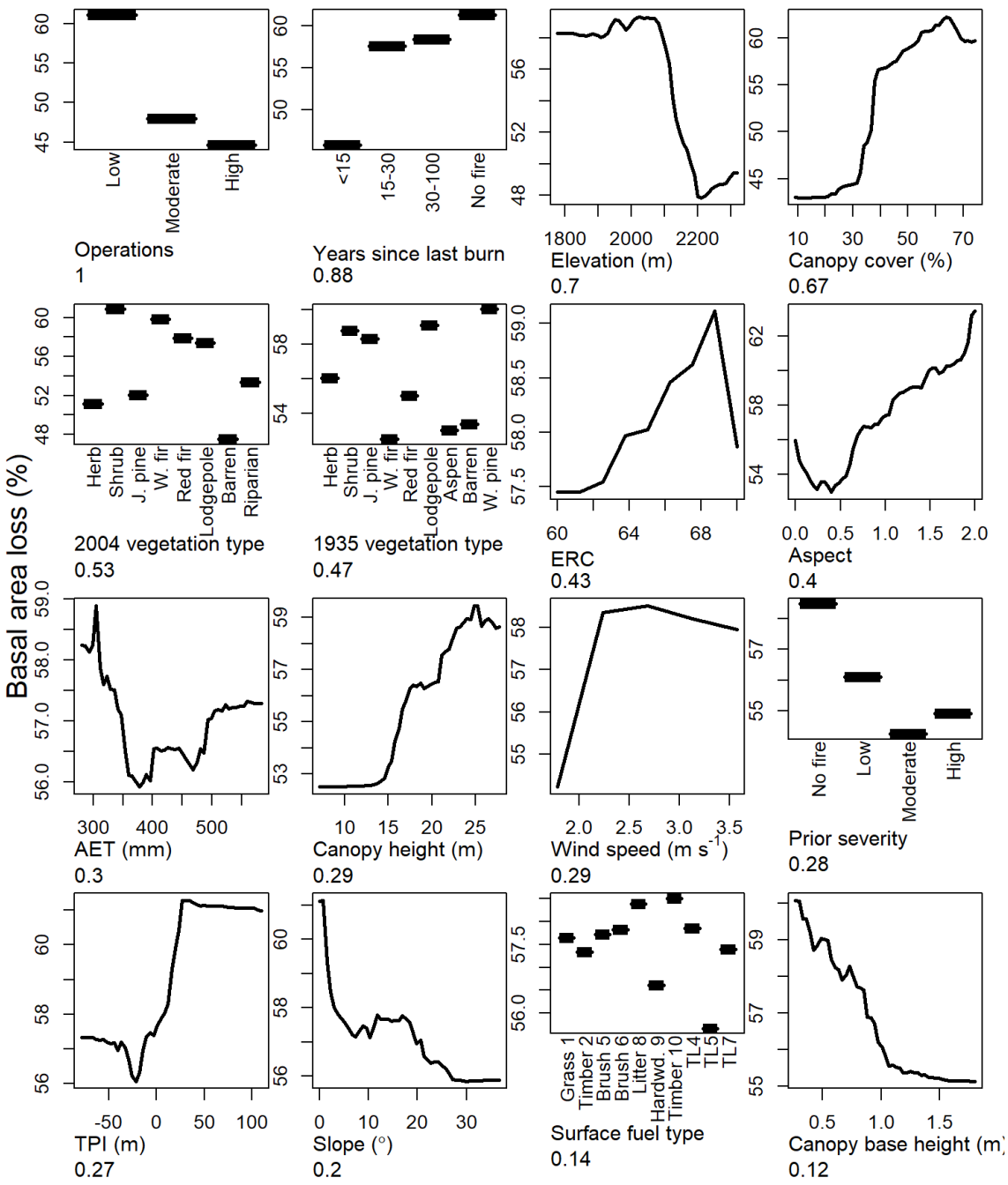

Fig. S8. Partial dependence plots showing relationships between basal area loss from the 2012 wildfire and individual predictor variables, based on a random forest model trained with samples spaced 330 m apart (pseudo-r^2 = 0.33). Variable importance is shown below each variable name.

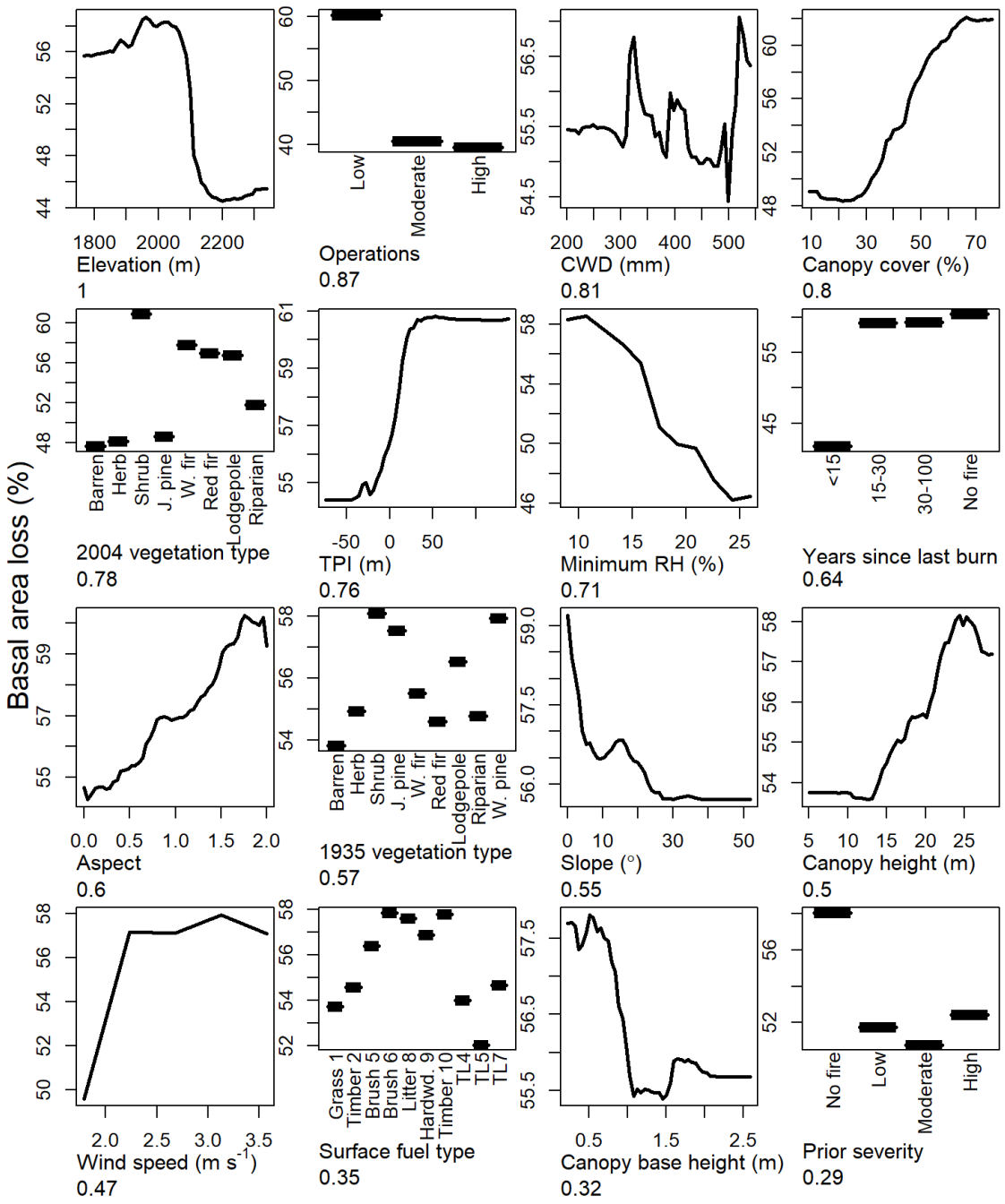

Fig. S9. Partial dependence plots showing relationships between basal area loss from the 2012 wildfire and individual predictor variables, based on a random forest model (pseudo-r^2 = 0.53) trained with samples spaced 120 m apart but including climatic water deficit (CWD) in the place of actual evapotranspiration. Variable importance is shown below each variable name.

References

Bjornstad ON (2020) 'ncf: Spatial Covariance Functions.' (R package version 1.2-9) https://cran.r-project.org/package=ncf.

Harris L, Taylor AH (2017) Previous burns and topography limit and reinforce fire severity in a large wildfire. *Ecosphere* **8**, Article e02019. doi:10.1002/ecs2.2019.

Kane VR, Cansler CA, Povak NA, Kane JT, Mcgaughey RJ, Lutz JA, Churchill DJ, North MP (2015) Mixed severity fire effects within the Rim fire: Relative importance of local climate, fire weather, topography, and forest structure. *Forest Ecology and Management* **358**, 62–79. doi:10.1016/j.foreco.2015.09.001.

Key CH, Benson NC (2006) Landscape Assessment (LA) Sampling and Analysis Methods. 'FIREMON Fire Eff. Monit. Invent. Syst.' (Ed DC Lutes) pp. 1–49. (General Technical Report RMRS-GTR-164-CD, USDA Forest Service Rocky Mountain Research Station: Ogden, UT, USA)

Koontz MJ, North MP, Werner CM, Fick SE, Latimer AM (2020) Local forest structure variability increases resilience to wildfire in dry western U.S. coniferous forests. *Ecology Letters* **23**, 483–494. doi:10.1111/ele.13447.

van Mantgem P, Schwartz M, Keifer M (2001) Monitoring fire effects for managed burns and wildfires: coming to terms with pseudoreplication. *Natural Areas Journal* **21**, 266–273. http://www.naturalareas.org/docs/v21_3_01_pp266_273.pdf.

Miller JD, Knapp EE, Key CH, Skinner CN, Isbell CJ, Creasy RM, Sherlock JW (2009) Calibration and validation of the relative differenced Normalized Burn Ratio (RdNBR) to three measures of fire severity in the Sierra Nevada and Klamath Mountains, California, USA. *Remote Sensing of Environment* **113**, 645–656. doi:10.1016/j.rse.2008.11.009.

Povak NA, Kane VR, Collins BM, Lydersen JM, Kane JT (2020) Multi-scaled drivers of severity patterns vary across land ownerships for the 2013 Rim Fire, California. *Landscape Ecology* **35**, 293–318. doi:10.1007/s10980-019-00947-z.

Taylor AH, Airey-Lauvaux C, Estes BL, Harris L, Skinner CN (2020) Spatial patterns of nineteenth century fire severity persist after fire exclusion and a twenty-first century wildfire in a mixed conifer forest landscape, Southern Cascades, USA. *Landscape Ecology* **35**, 2777–2790. doi:10.1007/s10980-020-01118-1.

Bjornstad O.N. 2019. Ncf: Spatial covariance functions. R package v. 1.2-8. https://CRAN.R-project.org/package=ncf.